Generation of intense isolated sub-40-as pulses from a coherent superposition state by quantum path control in the multicycle regime

Ji-Gen Chen,[1,*] Yu-Jun Yang,[2,†] Si-Liang Zeng,[3,‡] and Hua-Qiu Liang[1]
[1]*Department of Physics and Materials Engineering, Taizhou University, Taizhou 318000, China*
[2]*Institute of Atomic and Molecular Physics, Jilin University, Changchun 130012, China*
[3]*Institute of Applied Physics and Computational Mathematics, Beijing 100088, China*
(Received 20 October 2010; published 2 February 2011)

We theoretically investigate high-order harmonic generation and attosecond pulses by numerically solving the three-dimensional time-dependent Schrödinger equation from a helium ion in a two-color laser field, which is synthesized by adding a 1600-nm laser pulse to a multicycle 800-nm laser pulse. The numerical results show that the short quantum path selection and broadband continuum spectra are achieved by adjusting the relative phase between two laser pulses, and isolated attosecond pulses can be generated successfully. Compared with the case of He^+ ions from the 1*s* ground state, the emission efficiency of the continuous harmonics and the intensity of the isolated attosecond pulse are enhanced approximately thirteen orders of magnitude by preparing He^+ ions in a coherent superposition of the states 1*s* and 2*s*. Furthermore, the bandwidth of the continuum spectrum is further broadened by increasing the intensity of the 1600-nm laser pulse, and an intense 38-as isolated pulse with a bandwidth of 109 eV is straightforwardly obtained.

DOI: 10.1103/PhysRevA.83.023401 PACS number(s): 32.80.Rm, 42.50.Hz, 42.65.Ky

I. INTRODUCTION

The interaction of intense laser pulses with atomic and molecular systems results in the generation of high-order harmonic radiation in the extreme ultraviolet (XUV) and x-ray spectral ranges [1–3]. A typical high-order harmonic-generation (HHG) spectrum presents a fast decrease for the first few harmonics followed by a broad plateau of almost constant conversion efficiency, ending up with a sharp cutoff. Due to the special spectral structure, the HHG is a promising way to generate coherent x-rays in the "water window" (4.3–2.2 nm) and to produce attosecond pulses [1–3]. The mechanism of HHG can be well understood in terms of the semiclassical three-step model [4]: The electron first tunnels through the effective potential barrier formed by the atom and the laser field, then oscillates in the field and, finally, it may recombine to the ground state and emit a harmonic photon with energy equaling the ionization potential plus the kinetic energy of the recombining electron. It has been theoretically and experimentally demonstrated that an attosecond pulse train with a periodicity of half an optical cycle can be generated from HHG by a multicycle driving laser pulse [5–7], and every pulse in the train contains two peaks originating from the short and long quantum paths and characterized by an electron travel time in the continuum of approximately half and one optical cycles, respectively. For practical applications, an isolated attosecond pulse is preferable to a chain of attosecond pulses. Single-attosecond-pulse generation based on HHG has been realized by using a few-cycle laser pulse [8–10]. However, the continuum spectrum bandwidth is less than 20 eV, and the minimum duration of the isolated pulse is 250 as, which is greater than the characteristic time scale of electronic processes in atoms. By using a few-cycle laser pulse with the polarization gating technique, 130-as XUV pulses have been demonstrated experimentally [1]. However, the intensity of attosecond pulses produced in this scheme is limited by the low harmonic efficiency because only a fraction of the driving pulse energy is used for HHG.

Hence, a lot of effort has been devoted to generate intense isolated attosecond pulses. In the single-atom response, one of the most important methods of enhancing the harmonic efficiency and the attosecond pulse intensity is to prepare the initial state as a coherent superposition of two bound states. Coherently controlling a population transfer from an initial state to an arbitrary superposition between two bound states has attracted considerable interest in recent years. Many methods were proposed and employed, among which are three widely used schemes; that is, stimulated Raman adiabatic passage [11,12], chirped adiabatic passage [13,14], and temporal coherent control [15,16]. Recently, Zhdanovich *et al.* have experimentally investigated the population transfer using piecewise adiabatic passage from a single ground state to a superposition of excited states [17]. HHG enhancement from a coherent superposition state was first proposed by Gauthey *et al.* [18], Watson *et al.* [19] showed that a coherent superposition state can induce a dipole transition between the continuum and the ground states via the excited state responsible for the ionization, and Wang *et al.* [20] further demonstrated the evident advantages of using a coherent superposition state to obtain high-harmonic conversion efficiency. Zhai *et al.* [21] demonstrated the enhancement of HHG and intense 45-as isolated pulse generation using the coherent superposition state in a two-color laser field synthesized by a 12-fs pulse at 1600 nm and a 5-fs pulse at 800 nm; Zhang *et al.* [22] studied attosecond pulse generation from He^+ ions initially prepared in a coherent superposition using a 5-fs pulse at 800 nm in combination with a weak 64-fs pulse at 2400-nm, and an intense isolated attosecond pulse with a duration of 47 as was obtained; More recently, Wu *et al.* [23] used a

*tz501@yahoo.cn
†yangyj@jlu.edu.cn
‡zeng_siliang@iapcm.ac.cn

coherent superposition of the ground state and first-excited state as the initial state to generate an intense isolated 38-as pulse by combining a chirped 5-fs pulse at 800 nm with a 12-fs pulse at 1600 nm.

In this article, we also investigate the HHG enhancement and intense isolated attosecond pulse generation by using a coherent superposition in a two-color laser field. The HHG and attosecond pulse generation from the coherent superposition were studied by numerically solving the one-dimensional (1D) time-dependent Schrödinger equation (TDSE) in Refs. [21–23]. It has been shown that 1D calculations give the similar frequency dependence for HHG as three-dimensional (3D) simulations, but the harmonic efficiency is overestimated [24]. For achieving the more precise and accurate results, we investigate in this article isolated attosecond pulse generation based on 3D HHG calculations. Here, the multicycle 800-nm pulse is adopted, which should be much easier to obtain compared with the few-cycle 800-nm pulse generated by the state-of-the-art system in Refs. [21–23]. Our numerical results show that a broadband continuum spectrum can be produced in our two-color scheme, and an isolated attosecond pulse is generated successfully by eliminating the long quantum path. Compared with the case of He^+ ions from the $1s$ ground state, the emission efficiency of the continuous harmonics and the intensity of the isolated attosecond pulse are enhanced by about thirteen orders of magnitude by preparing He^+ ions in a coherent superposition of states $1s$ and $2s$. When we increase the intensity of the 1600-nm controlling laser pulse, the bandwidth of the continuum spectrum is further broadened, and an intense sub-40-as isolated pulse is straightforwardly generated. These results are analyzed based on the three-step model and the time-frequency analysis of HHG.

II. THEORETICAL FRAMEWORK

We use the 3D TDSE to describe the interaction between He^+ ions and a two-color laser field under the dipole approximation [atomic units (a.u.) are used throughout the article unless otherwise stated]:

$$i\frac{\partial}{\partial t}\psi(\vec{r},t) = \left[-\frac{1}{2}\nabla^2 + V_C(\vec{r}) - \vec{r}\cdot\vec{E}(t)\right]\psi(\vec{r},t), \quad (1)$$

where $V_C(\vec{r})$ is effective the Coulomb potential, and $E(t)$ is the linearly polarized electric field of the driving laser, which is chosen as the superposition of an intense multicycle 800-nm laser and a 1600-nm controlling pulse:

$$E(t) = E_0 f(t)\cos(\omega_0 t) + E_1 f(t-\tau_{\text{delay}}) \times \cos[\omega_1(t-\tau_{\text{delay}}) + \phi], \quad (2)$$

where E_0 and E_1 are the peak amplitudes of the electric fields of the two laser pulses, and ω_0 and ω_1 are the frequencies of the 800-nm and the 1600-nm pulses, respectively. The quantities ϕ and τ_{delay} are the relative phase and the time delay between the two lasers, respectively. The function $f(t) = \sin^2(\pi t/T)$ is the pulse envelope, the time t evolves from 0 to T, and $T = 10\,T_0$, corresponding to a duration of 10 fs full width at half maximum (FWHM), where $T_0 = 2.67$ fs is the period of the 800-nm laser pulse.

The TDSE (1) is efficiently solved by means of the well-known second-order split-operator method [25,26] implemented by the numerically exact fast transform between the grid and spectral representations [27,28]. In the grid representation, the radial coordinate is discretized using the Coulomb wave discrete variable representation (CWDVR) [27,28], and the angular dependence of the wave function is expanded in the Gauss-Legendre-Fourier grid [27,28]. In the spectral representation, the wave function is expanded in terms of the eigenfunctions of the field-free zero-order Hamiltonian. Once the wave function $\psi(\vec{r},t)$ is determined, the time-dependent induced-dipole acceleration can be given by Ehrenfest's theorem:

$$d_A(t) = \langle\psi(\vec{r},t)|-z/r^3 + \vec{E}(t)|\psi(\vec{r},t)\rangle, \quad (3)$$

and the HHG power spectrum is

$$P_A(\omega) = \left|\frac{1}{\sqrt{2\pi}}\int_0^t d_A(t)e^{-i\omega t}\,dt\right|^2. \quad (4)$$

To study the detailed spectral and temporal structures of HHG, we perform the time-frequency analysis by means of the wavelet transform [29]:

$$d_\omega(t) = \int d_A(t')\sqrt{\omega}W[\omega(t'-t)]\,dt'. \quad (5)$$

For the harmonic emission, a natural choice of the mother wavelet is given by the Morlet wavelet [30]:

$$W(x) = \frac{1}{\sqrt{\tau}}e^{ix}\exp\left(\frac{-x^2}{2\tau^2}\right). \quad (6)$$

By superposing several harmonics, an ultrashort pulse can be generated:

$$I(t) = \left|\sum_q a_q e^{iq\omega_0 t}\right|^2, \quad (7)$$

where

$$a_q = \int d_A(t)e^{-iq\omega_0 t}dt. \quad (8)$$

In this article, the initial state is prepared in the $1s$ ground state of the He^+ ion and a coherent superposition of the $1s$ and $2s$ states; that is,

$$\psi(\vec{r},t) = \frac{1}{\sqrt{2}}(|1s\rangle + e^{-i\delta}|2s\rangle). \quad (9)$$

We have changed the initial relative phase δ between the two states and found that the results have little change. Therefore, for the sake of simplicity, we take $\delta = 0$ throughout this article.

The time-dependent ionization probability is defined as

$$P_{\text{ion}}(t) = 1 - \sum_n |\langle n \mid \psi\rangle|^2, \quad (10)$$

where the summation runs over the bound states $|n\rangle$.

The underlying physical mechanism of HHG has been well explained in terms of the three-step model. If an electron is ionized at t_1, the corresponding emission time t_2 can be obtained by solving the following equation:

$$\int_{t_1}^{t_2}\int_{t_1}^{t} E(t)\,dt = 0. \quad (11)$$

The kinetic energy E_k of an electron ionized at t_1 and returning to the parent ion at t_2 can simply be expressed as

$$E_k = \frac{1}{2}\left[\int_{t_1}^{t_2} E(t)\,dt\right]^2. \tag{12}$$

By solving equations (11) and (12), we can investigate the electronic dynamics of the HHG process in the two-color field.

III. RESULTS AND DISCUSSION

We first study HHG from He^+ ions initially prepared in the 1*s* ground state exposed to a 10-fs fundamental laser pulse at 800 nm alone and a two-color laser field synthesized by the fundamental pulse and a 10-fs controlling pulse at 1600 nm, the intensities of which were 2.84×10^{14} and 3.16×10^{13} W/cm^2, respectively. As shown by the dashed red curve in Fig. 1, the harmonic spectrum of the fundamental pulse alone exhibits a plateau with the cutoff position at the 69th-order harmonic, which agrees with the cutoff formula $I_p + 3.2U_p$ [I_p is the ionization potential and $U_p = E_0^2/(4\omega_0^2)$ is the ponderomotive energy of the fundamental laser pulse]. One can see that the harmonics near the cutoff have separate sharp peaks caused by the multicycle accumulation, thus an attosecond pulse train with a periodicity of half the optical cycle can be generated by superposing these harmonics. By adding a relatively weak 10-fs, 1600-nm laser pulse to the intense 800-nm fundamental laser pulse and properly selecting the relative phase $\phi = 1.0\pi$ between the two lasers, the cutoff position of the harmonic spectrum is significantly extended to the 115th-order harmonic, as shown by the dash-dotted blue curve in Fig. 1. The cutoff frequency corresponds to the energy $I_p + 5.0U_p'$, where $U_p' = E_0^2/(4\omega_0^2) + E_1^2/(4\omega_1^2)$ is

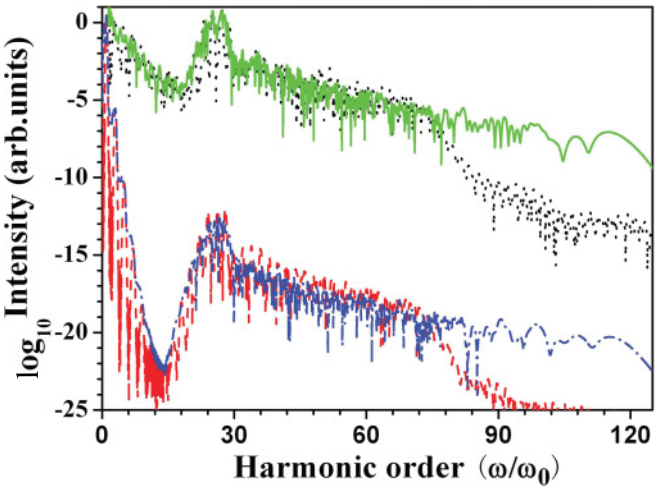

FIG. 1. (Color online) Harmonic spectra from He^+ ions initially prepared in the 1*s* ground state irradiated by a 10-fs, 800-nm laser field alone (dash red curve) and a two-color laser field (dash-dotted blue curve) synthesized by the 800-nm fundamental pulse and a 10-fs, 1600-nm pulse, respectively. Harmonic spectra from He^+ ions initially prepared in the coherent superposition of the states 1*s* and 2*s* irradiated by the fundamental laser field alone (dotted black curve) and the two-color laser field (solid green curve), respectively. The intensities of the 800-nm and 1600-nm pulses are 2.84×10^{14} and 3.16×10^{13} W/cm^2, respectively.

the ponderomotive energy for the two-color case, which is larger than the well-known value of $I_p + 3.2U_p$. Furthermore, one can notice that the harmonics are almost continuous and smooth near the cutoff position, which provides the potential probability generating an isolated attosecond pulse. As shown by the dashed-red and dash-dotted blue curves in Fig. 1 for the two cases of He^+ ions prepared in the ground state, the harmonic efficiencies are extremely low due to high ionization potential (54.4 eV) of He^+ ions.

In order to enhance the harmonic intensity, we also investigate HHG from He^+ ions initially prepared in a coherent superposition state irradiated by the fundamental laser pulse alone and the combined laser pulses. Here, the coherent state is prepared to the 1*s* and 2*s* superposition of states with equal population of 0.5. The harmonic spectra are presented by the dotted black and solid green curves in Fig. 1, respectively. Although the spectral structures of the two cases are almost the same as those of the dashed-red and dash-dotted blue curves, the plateaus of the superposition state are enhanced by approximately thirteen orders of magnitude in harmonic intensity. According to our calculations, a little more or less population of the 2*s* state than 0.5 (0.3–0.7) produces no distinct changes in the HHG spectra. Thus, it is possible to use the high-efficiency continuous spectrum shown in the solid green curve to obtain an intense attosecond pulse.

To more clearly understand the enhancement of the harmonic emission and the generation of the continuum spectra, we calculate the ionization probability and investigate the HHG process by the semiclassical three-step model. The dotted black curves in Figs. 2(a) and 2(b) exhibit the electric fields of the one-color laser pulse and two-color laser pulse with $\phi = 1.0\pi$, respectively. The ionization probability is shown by the solid red curve in Fig. 2 when the initial state is prepared as the coherent superposition state. The insets in Fig. 2 show the ionization probability from the initial state prepared to the ground state. It can be observed that the ionization probability from the former is increased in excess of three orders of magnitude compared with that from the latter. Considering the stimulated property [31] of the recombination in laser fields, the ground and continuum states in the former have large a population and harmonic emission with high efficiency can be obtained, as shown by the dotted black and solid green curves in Fig. 1. In our simulation, due to the intensity of the laser pulse being much lower than the saturation intensity of He^+ ions, the population of the continuum state in the latter is very small and so is the harmonic efficiency, as shown by the dashed-red and dash-dotted blue curves in Fig. 1. These results testify that the large population of the continuum state is mainly attributed to the excited state and that the harmonics with high efficiency can be achieved by using a coherent superposition state.

Next, we investigate the electronic dynamics of the HHG process with the three-step model. Figures 3(a) and 3(b) show the dependences of harmonic order on the ionization time (blue circles) and the emission time (red triangles) in the one-color laser field alone and the two-color laser field, respectively. From Fig. 3(a), one can see that the electrons ionized near peaks P_1, P_2, and P_3 in the one-color laser field contribute to the harmonics in the end of the plateau, and two radiations for each harmonic periodically occur every half optical cycle

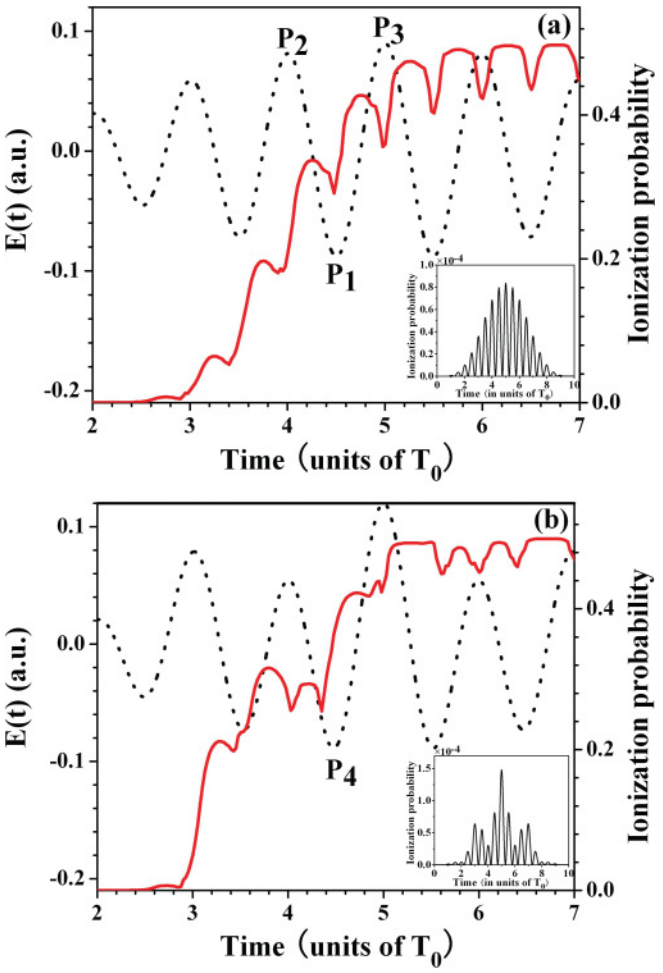

FIG. 2. (Color online) Electric field (dotted black curve) of (a) the 10-fs, 800-nm laser field alone and (b) the two-color laser field. The parameters are the same as in Fig. 1. The solid red curve presents the time dependence of the ionization probability when He^+ ions are initially prepared as a coherent superposition. The inset shows the time dependence of the ionization probability when He^+ ions are initially prepared as the ground state.

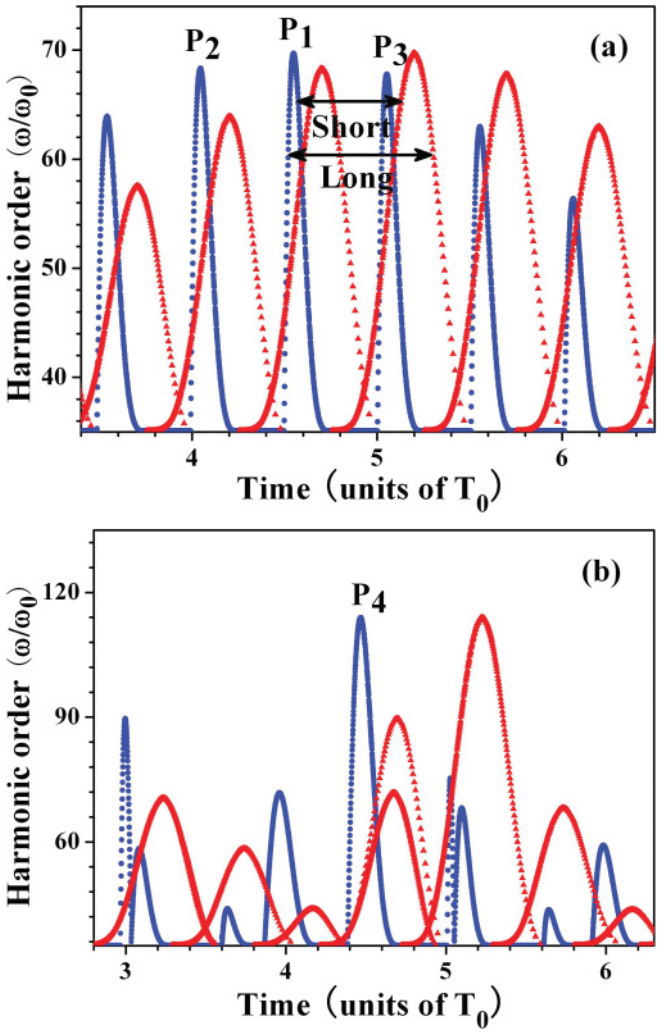

FIG. 3. (Color online) Dependence of harmonic order on the ionization time (blue circles) and the emission time (red triangles) in (a) the 10-fs, 800-nm laser field alone and (b) the two-color laser field. The parameters are the same as in Fig. 1.

because of the symmetry of the one-color laser field. Hence, the superposition of these harmonics near the cutoff region will generate an attosecond pulse train, and every pulse in the train contains two peaks originating from two quantum paths. The one with earlier ionization and later recombination time is called the long path, and the one with later ionization and earlier recombination time is called the short path. As shown in Fig. 3(b), the highest-order harmonics from 90 to 115 are generated due to the electrons being ionized near peak P_4 of the two-color laser field, and only two quantum paths contribute to these harmonics. Electrons with the short paths are mainly ionized from 4.47 optical cycles (o.c.) of the fundamental laser to 4.72 o.c., and electrons with the long paths are mainly ionized from 4.38 to 4.47 o.c. However, the ionization rates for the short paths are much higher than those for the long paths, which can be found from the red curve in Fig. 2(b). In addition, electrons with long paths travel a longer time in the continuous state, which results in a lower harmonic efficiency due to the quantum diffusion. Therefore, the harmonic efficiency for the short path is higher than that for the long path. This result indicates that the single short quantum path can be selected by using the 1600-nm laser pulse in our two-color scheme.

In order to obtain a deeper insight for HHG generation, the emission times of the harmonics in the case of the coherent superposition state are investigated by the wavelet time-frequency analysis method [29,30]. Figure 4(a) presents the time-frequency distribution of the HHG corresponding to the dotted black curve in Fig. 1. One can clearly see that three main peaks P_1, P_2, and P_3 contribute to the harmonics near the cutoff region. For each peak, the positive- and negative-sloped branches correspond to the short and long paths, which have different emission times. Therefore, the superposition of these harmonics in the cutoff region will result in two radiation pulses. This result is consistent with that analyzed based on the three-step model in Fig. 3(a). Figure 4(b) also shows the time-frequency diagram of the HHG corresponding to the solid green curve in Fig. 1. It can be seen that there is only one peak (marked P_4) contributing to the highest-order harmonics. Furthermore, in the peak P_4, the

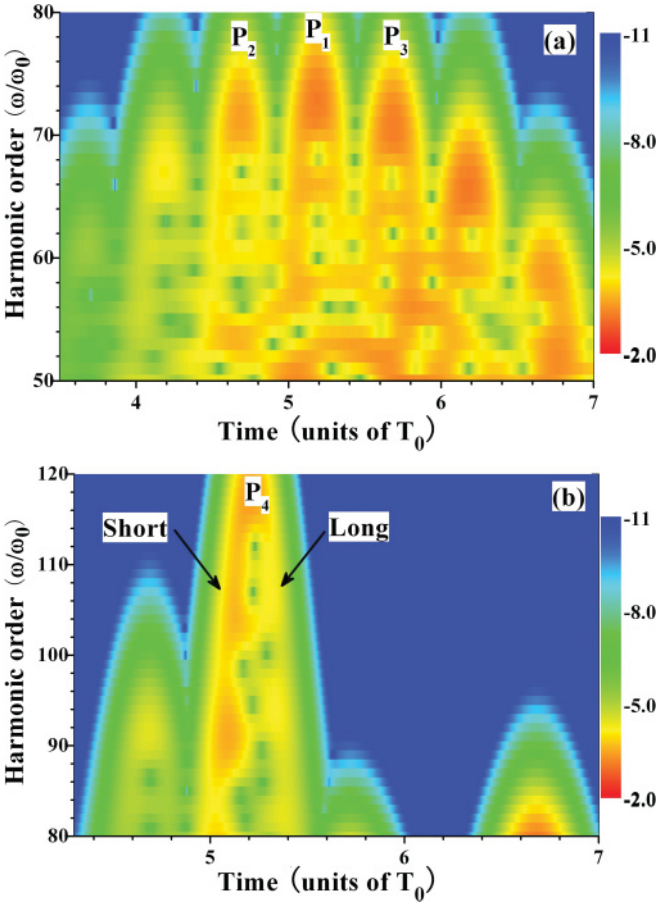

FIG. 4. (Color online) Time-frequency distributions of the HHG corresponding to the dotted black (a) and solid green curves (b) in Fig. 1.

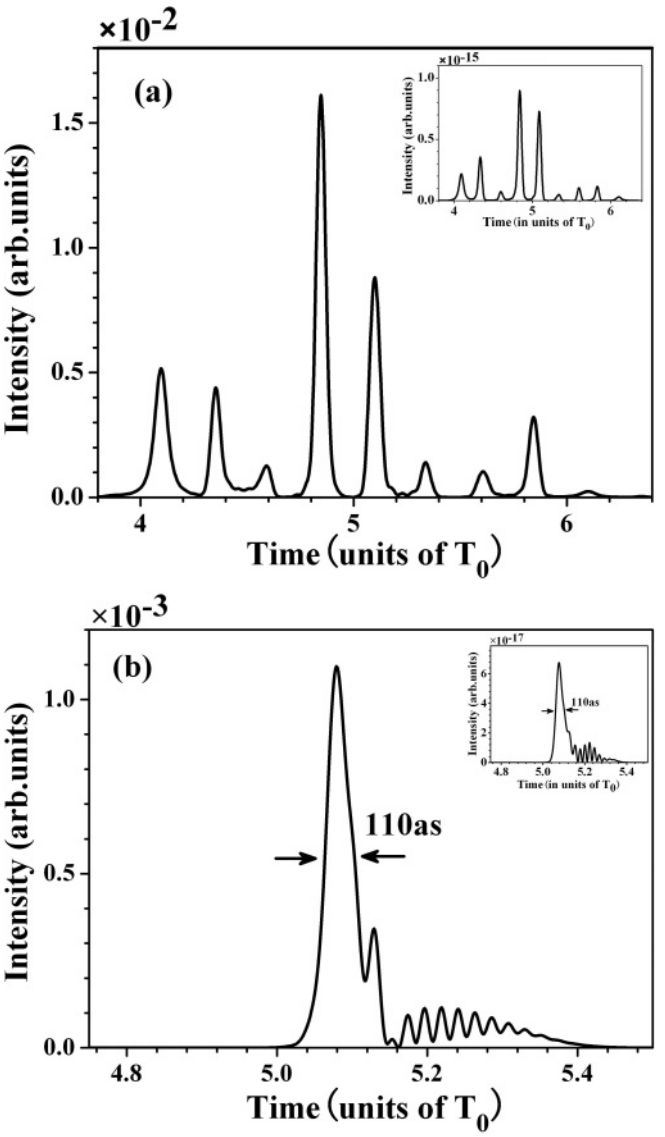

FIG. 5. Temporal profiles of the attosecond pulses from He^+ ions in the coherent superposition state: (a) by superposing the harmonics from the 67th to 77th order in the one-color field, (b) by superposing the harmonics from the 101st to123rd order in the two-color field. The insets show the temporal profiles of the attosecond pulses from He^+ ions in the ground state.

harmonic intensity of the short path is higher than that of the long path, and the highest-order harmonics are emitted almost in phase, thus an isolated attosecond pulse will be generated by superposing these synchronous harmonics. These results also are consistent with those discussed above in terms of the ionization probability and the three-step model.

In the following, we investigate the attosecond pulse generation in both cases of the one-color and two-color laser fields. The temporal profile of the attosecond pulse can be produced by simply making an inverse Fourier transformation of the HHG spectrum. Figures 5(a) and 5(b) present the attosecond pulses generated from He^+ ions initially in the coherent superposition state. For the case of the one-color laser pulse, the harmonics selected to synthesize the attosecond pulse are from the 67th to 77th order near the cutoff; one can see clearly that there are two adjacent attosecond bursts every half optical cycle, as shown in Fig. 5(a). This result agrees well with that from the time-frequency diagram in Fig. 4(a), in which it can be found that the first and second attosecond pulses originate from the contribution of the short and long paths, respectively. Furthermore, the above result is consistent with those reported for attosecond pulse trains generation by the multicycle laser pulse [5–7]. Figure 5(b) shows the temporal profile of the attosecond pulse by filtering the 101st-123rd harmonic from the continuous spectrum in the two-color laser field; a single 110-as pulse with several small satellites is obtained. It is further demonstrated that an isolated attosecond pulse can be generated by adding a weak 1600-nm laser to the fundamental pulse. Moreover, the intensities of the attosecond pulses from the coherent superposition state are enhanced by about thirteen orders of magnitude in comparison with the case of the insets in Fig. 5, which present the temporal profiles of the attosecond pulses obtained from He^+ ions initially prepared in the ground state.

In the above calculations, the intensity of the controlling field is about 11% of the fundamental laser pulse. To further shorten the attosecond pulse duration, we propose an efficient method to significantly extend the bandwidth of the continuous harmonic spectrum by increasing the peak intensity of the 10-fs, 1600-nm controlling laser pulse. The solid red curve

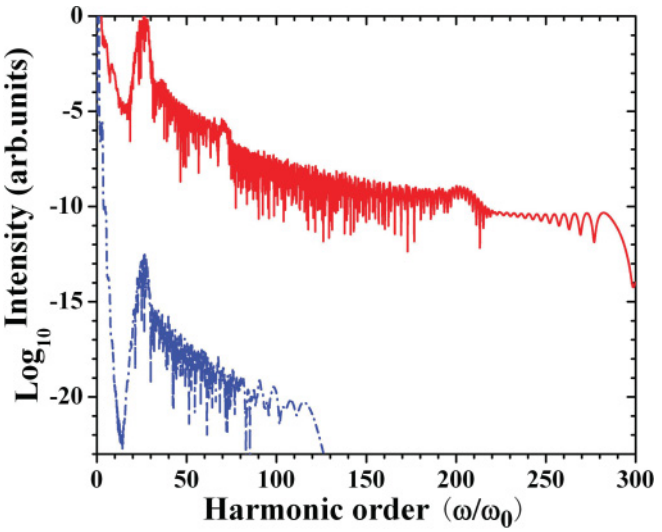

FIG. 6. (Color online) Solid red curve shows the harmonic spectrum from He^+ ions initially prepared in the coherent superposition irradiated by a 10-fs, 800-nm pulse and a 10-fs, 1600-nm pulse with the same peak intensities of 2.84×10^{14} W/cm^2. Harmonic spectra from He^+ ions initially prepared in the ground state (dash-dotted blue curve) irradiated by the two-color laser field in combination with a 10-fs, 800-nm pulse and a 10-fs, 1600-nm pulse; their peak intensities are 2.84×10^{14} and 3.16×10^{13} W/cm^2, respectively.

in Fig. 6 presents the harmonic spectrum from He^+ ions initial prepared in the coherent superposition irradiated by a 10-fs, 800-nm pulse and a 10-fs, 1600-nm pulse with equal peak intensities of 2.84×10^{14} W/cm^2. Note that an available few-cycle 1- to 5-μm laser pulse with intense intensity can be obtained by the optical parametric amplifier (OPA) [32]. For comparison, Fig. 6 also shows the HHG spectrum corresponding to the dash-dotted blue curve in Fig. 1. As shown in Fig. 6, the continuous harmonic range of the solid red

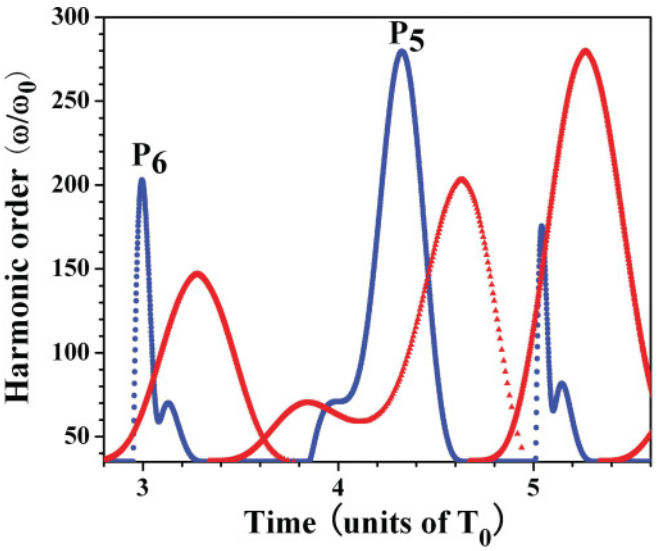

FIG. 7. (Color online) Dependence of harmonic order on the ionization time (blue circles) and the emission time (red triangles) in the two-color laser field. The parameters are same as those of the solid red curve in Fig. 6.

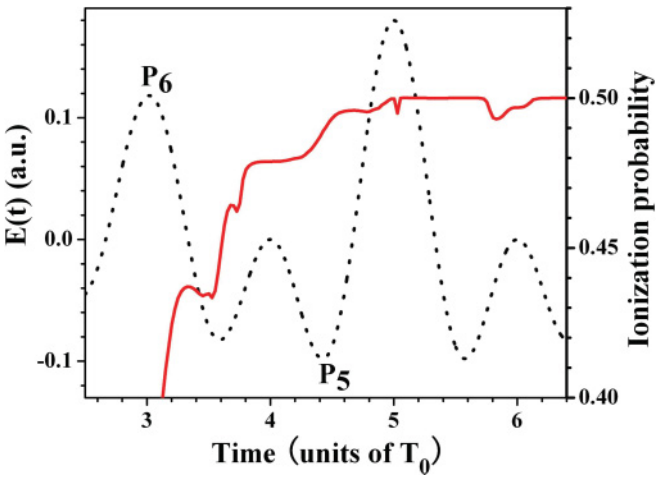

FIG. 8. (Color online) Electric field (dotted black curve) of the two-color laser field, the parameters are same with those of the solid red curve in Fig. 6. The solid red curve presents the time dependence of the ionization probability when He^+ ions are initially prepared as a coherent superposition.

curve is about from the 210th to 280th order, corresponding to a bandwidth of 109 eV, which is approximately 78 eV broader than that for the case of the solid green curve in Fig. 1. Figure 7 shows the dependence of harmonic orders to the ionization and recombination times in the two-color field. When the intensity of the controlling field is increased to the same as that of the driving laser pulse, the highest and the second-highest harmonics (marked P_5 and P_6 in Fig. 7) are enhanced to the 280th and 203rd order, which are consistent with the two cutoff positions in the harmonic spectrum. Moreover, only two electron paths generate the harmonics above the 203rd; electrons with the long paths are mainly ionized from 4.227 to 4.326 o.c., and electrons with the short paths are mainly ionized from 4.326 to 4.421 o.c. Figure 8 presents the time dependence of the ionization probability (solid red curve) and the electric field (dotted black curve) of the two-color laser field, the parameters of which are same with those of the solid red curve in Fig. 6. It can be observed from this figure, for the harmonics near the peak P_5, that the ionization rate

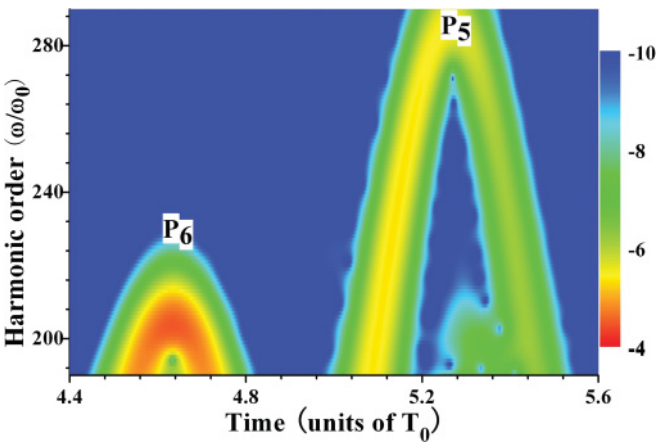

FIG. 9. (Color online) Time-frequency distribution of the HHG corresponding to the solid red curve in Fig. 6.

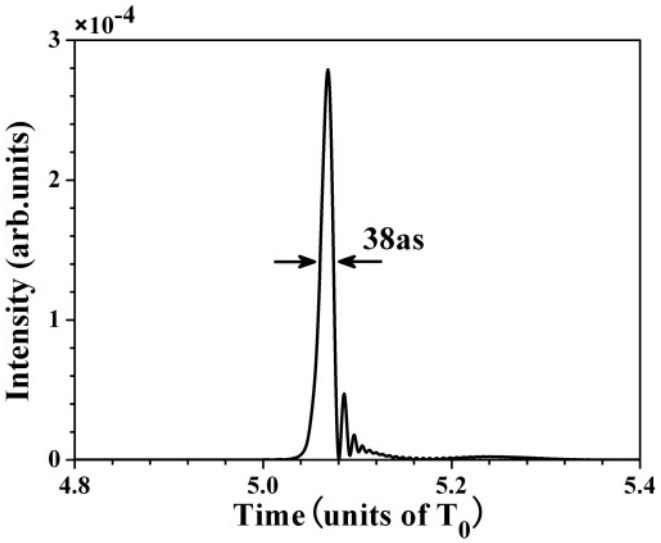

FIG. 10. Temporal profile of the isolated attosecond pulse from He^+ ions prepared in a coherent superposition state. The harmonics from the 213rd to 283rd are selected. Other parameters are the same as those of the solid red curve in Fig. 6.

of the short path is higher than that of the long path. The time-frequency diagram shown in Fig. 9 further confirms that the selection of the short quantum path can be achieved in this case. By superposing the 213rd–283rd harmonic in the continuous region, an intense isolated 38-as pulse with high signal-to-noise ratio is straightforwardly obtained without any phase compensation, as shown in Fig. 10.

IV. CONCLUSIONS

In conclusion, we theoretically investigate HHG and isolated attosecond pulse generation when He^+ ions are irradiated by a multicycle 800-nm laser pulse in combination with a controlling 1600-nm laser pulse. It is shown that the broadband continuum spectrum can be achieved in our two-color field, and an isolated attosecond pulse is generated successfully via suppressing the long quantum path. Moreover, the continuous harmonics with higher emission efficiency is obtained by preparing He^+ ions in a coherent superposition of the states $1s$ and $2s$, and the intensity of the attosecond pulse is correspondingly enhanced by thirteen orders of magnitude compared with the case of He^+ ions in the ground state.

Finally, we would like to point out that our scheme has several characteristics. First, the 800-nm pulse used here is multicycle one, and so should be much easier to obtain compared with the few-cycle pulses, which are usually adopted in two-color quantum path control schemes [21–23,33–37]. Second, our simulation shows that the value of the time delay can be varied as much as $\pm 0.15\pi$ to keep the isolated sub-50-as pulse generation with the side peak less than 23% of the main peak intensity. Third, the continuous spectra and broadband sub-50-as isolated pulses can be generated by the controlling laser pulse with an intensity ranging from 1.7×10^{14} to 4.3×10^{14} W/cm^2. The above characteristics indicate that it is experimentally feasible to obtain efficient isolated attosecond pulses with our scheme. In addition, the intensity 2.84×10^{14} W/cm^2 of the controlling laser pulse has the optimal value to simultaneously ensure the wider bandwidth and the higher efficiency of the continuum harmonics, and an intense 38-as isolated pulse with a bandwidth of 109 eV is directly generated without phase compensation in this case. Such an ultrashort pulse allows one to manipulate the electronic dynamics more powerfully with an unprecedented time resolution.

ACKNOWLEDGMENTS

This work was supported by the National Natural Science Foundation of China under Grant No. 10604021 and No. 10904006, and the Science and Technology Fund of China Academy of Engineering Physics (Grant No. 2009B0102011). We acknowledge the High Performance Computing Center of Jilin University for supercomputer time. Y.J.Y. acknowledges the support of the Fundamental Research Funds for the Central Universities (Grant No. 200903368) and the National Natural Science Foundation of China (Grant No. 11034003).

[1] G. Sansone *et al.*, Science **314**, 443 (2006).
[2] P. B. Corkum and F. Krausz, Nature Physics **3**, 381 (2007).
[3] F. Krausz and M. Ivanov, Rev. Mod. Phys. **81**, 163 (2009).
[4] P. B. Corkum, Phys. Rev. Lett. **71**, 1994 (1993).
[5] P. M. Paul *et al.*, Science **292**, 1689 (2001).
[6] T. Pfeifer, L. Gallmann, M. J. Abel, D. M. Neumark, and S. R. Leone, Opt. Lett. **31**, 975 (2006).
[7] W. Cao, P. X. Lu, P. F. Lan, X. L. Wang, and G. Yang, Opt. Express **15**, 530 (2007).
[8] R. Kienberger *et al.*, Nature (London) **427**, 817 (2004).
[9] M. Hentschel *et al.*, Nature (London) **414**, 509 (2001).
[10] A. Baltuska *et al.*, Nature (London) **421**, 611 (2003).
[11] K. Bergmann, H. Theuer, and B. W. Shore, Rev. Mod. Phys. **70**, 1003 (1998); N. V. Vitanov *et al.*, Annu. Rev. Phys. Chem. **52**, 763 (2001).
[12] R. G. Unanyan, B. W. Shore, and K. Bergmann, Phys. Rev. A **59**, 2910 (1999); F. Vewinger, M. Heinz, R. G. Fernandez, N. V. Vitanov, and K. Bergmann, Phys. Rev. Lett. **91**, 213001 (2003); X. H. Yang and S. Y. Zhu, Phys. Rev. A **78**, 023818 (2008).
[13] J. S. Melinger *et al.*, J. Chem. Phys. **101**, 6439 (1994); B. Y. Chang *et al.*, Phys. Rev. A **64**, 033420 (2001).
[14] S. A. Malinovskaya and V. S. Malinovsky, Opt. Lett. **32**, 707 (2007); J. Mod. Opt. **55**, 3101 (2008).
[15] R. N. Zare, Science **279**, 1875 (1998); S. Chu, Nature (London) **416**, 206 (2002).
[16] V. Engel and H. Metiu, J. Chem. Phys. **100**, 5448 (1994); V. Blanchet *et al.*, Phys. Rev. Lett. **78**, 2716 (1997); X. H. Yang, Z. R. Sun, and Z. G. Wang, Phys. Rev. A **76**, 043417 (2007).
[17] S. Zhdanovich, E. A. Shapiro, J. W. Hepburn, M. Shapiro, and V. Milner, Phys. Rev. A **80**, 063405 (2009).

[18] F. I. Gauthey, C. H. Keitel, P. L. Knight, and A. Maquet, Phys. Rev. A **52**, 525 (1995).
[19] J. B. Watson, A. Sanpera, X. Chen, and K. Burneet, Phys. Rev. A **53**, R1962 (1996).
[20] B. Wang, T. Cheng, X. Li, P. Fu, S. Chen, and J. Liu, Phys. Rev. A **72**, 063412 (2005).
[21] Z. Zhai, R. F. Yu, X. S. Liu, and Y. J. Yang, Phys. Rev. A **78**, 041402(R) (2008).
[22] G. T. Zhang and X. S. Liu, J. Phys. B: At. Mol. Opt. Phys. **42**, 125603 (2009).
[23] J. Wu, G. T. Zhang, C. L. Xia, and X. S. Liu, Phys. Rev. A **82**, 013411 (2010).
[24] S. C. Rae, X. Chen, and K. Burnett, Phys. Rev. A **50**, 1946 (1994).
[25] M. D. Feit and J. A. Fleck, J. Chem. Phys. **78**, 301 (1983).
[26] M. D. Feit, J. A. Fleck, and A. Steiger, J. Comput. Phys. **47**, 412 (1982).
[27] S. L. Zeng, S. Y. Zou, and J. Yan, Chin. Phys. Lett. **26**, 053202 (2009).
[28] J. G. Chen, S. L. Zeng, and Y. J. Yang, Phys. Rev. A **82**, 043401 (2010).
[29] X. M. Tong and Sh. I. Chu, Phys. Rev. A **61**, 021802(R) (2000).
[30] X. Chu and Sh. I. Chu, Phys. Rev. A **64**, 021403(R) (2001).
[31] A. Pukhov, S. Gordienko, and T. Baeva, Phys. Rev. Lett. **91**, 173002 (2003).
[32] C. Vozzi, F. Calegari, E. Benedetti, S. Gasilov, G. Sansone, G. Cerullo, M. Nisoli, S. De Silvestri, and S. Stagira, Opt. Lett. **32**, 2957 (2007).
[33] P. F. Lan, P. X. Lu, W. Cao, Y. H. Li, and X. L. Wang, Phys. Rev. A **76**, 011402(R) (2007).
[34] Z. Zeng, Y. Cheng, X. Song, R. Li, and Z. Xu, Phys. Rev. Lett. **98**, 203901 (2007).
[35] Z. Zhai and X. S. Liu, J. Phys. B: At. Mol. Opt. Phys. **41**, 125602 (2008).
[36] W. Y. Hong, P. X. Lu, P. F. Lan, Z. Y. Yang, Y. H. Li, and Q. Liao, Phys. Rev. A **77**, 033410 (2008).
[37] S. F. Zhao, X. X. Zhou, P. C. Li, and Z. J. Chen, Phys. Rev. A **78**, 063404 (2008).